Molecular-matched materials for anticancer drug delivery and imaging

Aim: In this study, we aim to construct nanoformulation with high-cargo loading and controlled serum kinetics. **Materials & methods:** Molecular-matched materials (MMMs) are established through the conjugation of the functional moiety to a molecule representative of the nanoparticle's core. Molecular-matched nanoemulsions and liposomes were prepared using MMMs. **Results:** This technique based on MMMs even allows us to efficiently load either hydrophobic or hydrophilic moieties into a hydrophobic core of the nanoparticles. MMMs-based nanoparticles showed marked improvement in serum pharmacokinetics and anticancer effect. **Conclusion:** The desired performance can be achieved when the hydrophobic anchor of the PEG derivatives and the moiety conjugated to the therapeutic (or imaging) agents are molecularly identical to the core.

Keywords: imaging • long circulation • molecular-matched nanoparticles • paclitaxel • PEGylation

Dun Wang[‡,1], Qiang Fu[‡,2], Jingling Tang[3], Michael Hackett[4], Yongjun Wang*[,2] & Feng Liu[§,¶,4]

[1]Key Laboratory of Structure-Based Drug Design & Discovery, Ministry of Education, Shenyang Pharmaceutical University, Shenyang, 110016, China
[2]Department of Pharmaceutics, School of Pharmacy, Shenyang Pharmaceutical University, Shenyang, 110016, China
[3]School of Pharmacy, Harbin Medical University, Harbin, 150081, China
[4]Division of Molecular Pharmaceutics, Eshelman School of Pharmacy, University of North Carolina at Chapel Hill, Chapel Hill, NC 27599, USA
*Author for correspondence:
Tel.: +86 24 23986325
Fax.: +86 24 23986325
wangyjspu@163.com
[‡]Authors contributed equally
[§]Deceased
[¶]Dedicated to the memory of Professor Feng Liu, PhD, 1955–2014

Nanocarriers designed with hydrophobic cores are often useful for delivering hydrophobic drugs but are highly incompatible with hydrophilic imaging probes. Additionally, highly crystalline hydrophobic drugs, such as paclitaxel (PTX), may also be incompatible with these particles. This leads to issues with cargo selectivity and loading efficiency. Other common issues with nanocarriers are uncontrolled cargo release or rapid pharmacokinetic (PK) clearance. Great efforts have been made to remedy these problems; however, no carrier has effectively managed all these issues [1–5]. While many different formulations have been applied to PTX, there has been very little success thus earning it the description 'brickdust' [6]. As to PTX formulation, only Taxol and Abraxane were approved by the US FDA for cancer therapy, but both have some limitations. Taxol requires the use of Cremophor-EL at a ratio of PTX to surfactant of 1/90 (w/w); this dose of Cremophor-EL is well documented to cause serious side effects, including hypersensitivity reactions, nephrotoxicity, cardio-

toxicity and neurotoxicity [7,8]. Although Abraxane has several practical advantages over Taxol, such as the significant reduction of toxicity and the increase in the efficiency of PTX loading, Abraxane did not improve the PK of PTX [9,10]. Additionally, there is no evidence that either Abraxane or Taxol can overcome multiple drug resistance (MDR) in cancer. Many efforts have been made to improve the PK of PTX; for example, Sonus Pharmaceuticals developed an injectable, PEGylated PTX nanoemulsion (NE) with vitamin E (VE) as the oil-core. However, this NE failed in a pivotal phase III study conducted in breast cancer patients [11]. Letchford K and Burt HM designed copolymers composed of higher molecular weight hydrophobic blocks that form nanoparticles (NPs). These so-called 'frozen core' particles were expected to better retain PTX, thus leading to prolonged circulation of the drugs. Unfortunately, their results indicated PTX was still eliminated from the blood rapidly due to instability of the carrier upon injection [12]. Therefore, the rational design of NPs should

be made based on a sound understanding of the problems that could arise from poor compatibility between cargo and the core of the NPs.

In order to improve the compatibility between the cargo and the core of the NPs, we developed molecular-matched NPs based on our technique of molecular-matched materials (MMMs). These materials were synthesized by conjugating a functional molecule to a molecule representative of the core of the NPs; functional molecules include drugs, fluorescent imaging probes or PEG (Figure 1). The molecular-matched NPs were then formulated using MMMs. We hypothesized that the solubility of these MMMs would be increased due to more favorable interactions with the particle core, which would effectively anchor the functional molecules to the particle. This could provide the benefit of preventing premature drug release, and the PEG stabilization could allow prolonged PK profiles for improving therapeutic outcomes. We then applied the MMMs to create molecular-matched NPs including NEs and liposomes. These nanoparticles were then examined for their ability to deliver either molecular-matched or mismatched agents, hydrophobic drugs, PEG derivatives and hydrophilic fluorescent imaging probes.

Materials & methods

Materials

PTX (^{3}H-labeled) was purchased from LC Laboratories (MA, USA). D-α tocopheryl polyethylene glycol 1000 succinate (TPGS) was purchased from Eastman (Anglesey, UK). 1,2-dioleoyl-*sn*-glycero-3-phosphocholine, 1,2-distearoyl-*sn*-glycero-3-phosphoethanolamine-N-[amino(polyethylene glycol)-2000] (DSPE-PEG2000) and 1,2-distearoyl-*sn*-glycero-3-phosphoethanolamine-N-[poly(ethylene glycol)2000-N'-carboxyfluorescein] (DSPE-PEG2000-CF) were purchased from Avanti Polar Lipids. Sulforhodamine acid chloride (SRB), (+)-α-tocopherol (VE), D-α-tocopherol succinate and linoleic acid (LA) were purchased from Sigma-Aldrich (MO, USA). PTX conjugated compounds [13,14], SRB conjugated compounds [15], and VE PEGylated compounds [16,17] were synthesized by our previous methods or other literatures.

Solubility measurements

The solubility of PTX, VE-PTX and LA-PTX in VE and LA was determined using a saturation method. Briefly, excess PTX or PTX conjugates (trace amount of ^{3}H-PTX or ^{3}H-PTX-LA was mixed inside) in chloro-
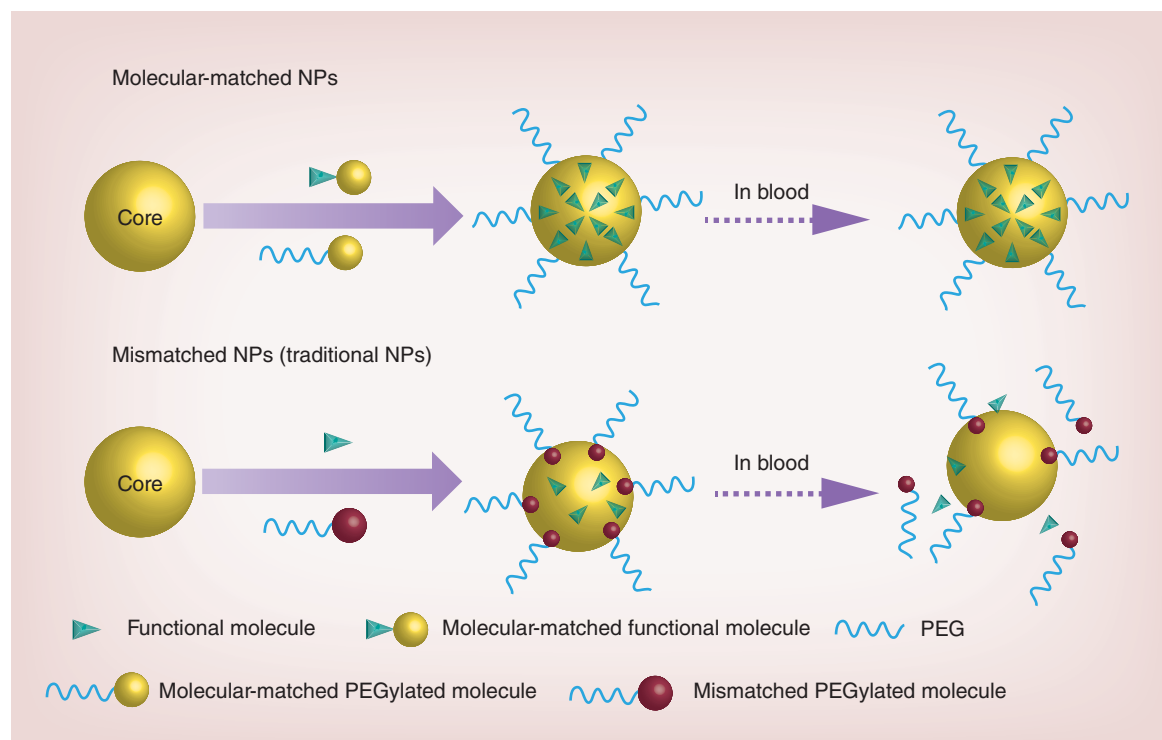

Figure 1. Schematic representation of the development of tunable nanoparticles based on molecular-matched materials. The molecular-matched NPs that are assembled through the molecular-matched materials achieve much higher drug-loading efficiency compared with the mismatched NPs (traditional NPs). Upon entry into circulation, the molecular-matched conjugates are stabilized due to the strong interaction with the lipid core, which ensures the efficient delivery of the loaded drugs to the targeted tumor tissues. In the case of the mismatched NPs (traditional NPs), cargo and PEGylated molecules will dissociate and be eliminated by the liver, spleen or kidneys. NP: Nanoparticle.
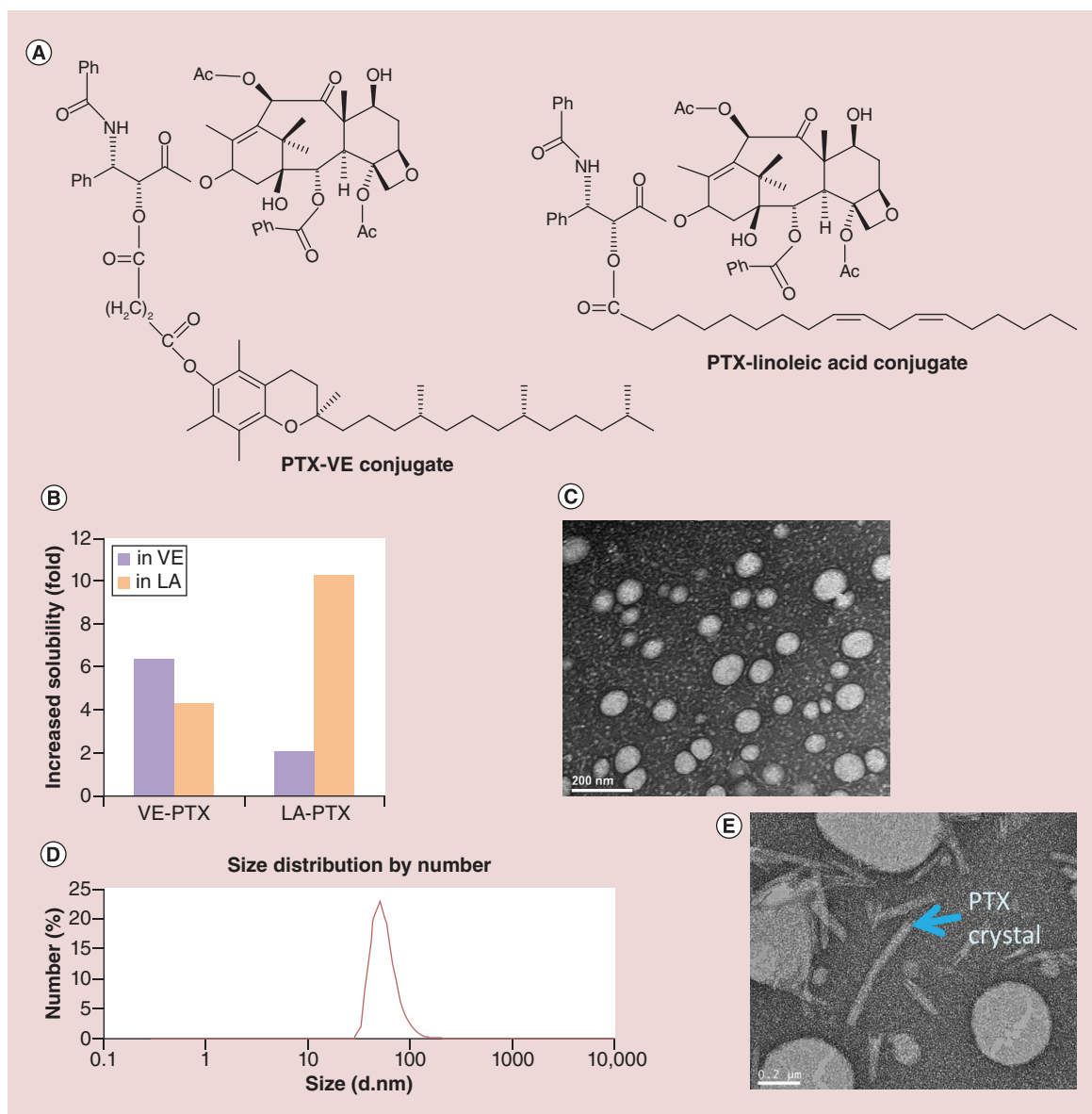
Figure 2. The development of vitamin E-paclitaxel molecular-matched nanoemulsions. (A) The molecular structure of VE-PTX and LA-PTX. (B) Increased folds of solubility of VE-PTX and LA-PTX compared with free PTX. (C) TEM images of VE-PTX NEs (VE-PTX/VE/TPGS = 160/900/360, w/w). (D) The average particle size and size distribution of VE-PTX NEs (pH 7.4 PBS as solvent, 1.6 mg/ml VE-PTX NEs were diluted about 50-fold) were determined by quasielastic laser light scattering with a Malvern Zetasizer at 25°C (n = 3). (E) TEM images of PTX NEs (PTX/VE/TPGS = 10/900/360, w/w).
LA-PTX: Linoleic acid-paclitaxel; NE: Nanoemulsion; TEM: Transmission electron microscopy; TPGS: D-α tocopheryl polyethylene glycol 1000 succinate; VE-PTX: Vitamin E-paclitaxel.

form was mixed with a VE or LA chloroform solution. The chloroform was then evaporated using a nitrogen gas flow keeping the mixtures under a vacuum in a desiccator for 12 h. The mixtures were centrifuged for 3 h at a speed of 10,000 rpm and the supernatant oil was extracted. The same method was applied to determine the solubility of SRB, VE-SRB and LA-SRB in VE or LA. The amounts of PTX and VE-PTX were quantified using a liquid scintillation analyzer, and LA-PTX was quantified using HPLC. SRB, VE-SRB

and LA-SRB were quantified using a fluorescence spectrophotometer (λ_{ex} = 560 nm, λ_{em} = 584 nm). ^{3}H-PTX and ^{3}H-PTX-VE were used to detect the solubility of PTX and VE-PTX, and the solubility of LA-PTX was detected using HPLC [13].

Preparation of molecular-matched nanoparticles

All molecular-matched NPs were prepared using the same preliminary treatment followed by different post-
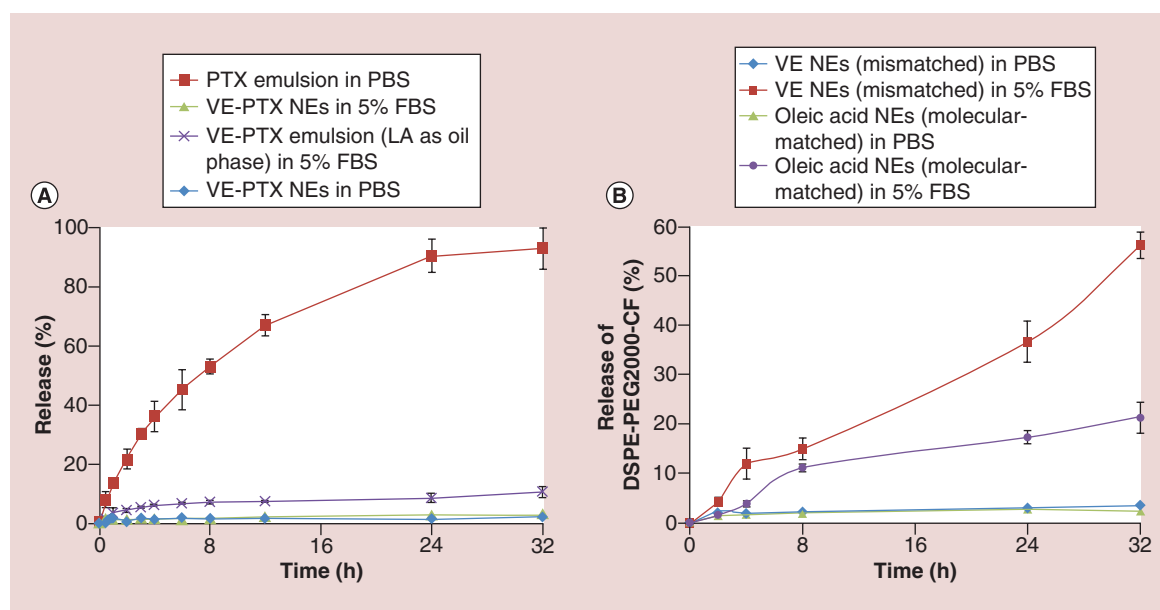
Figure 3. *In vitro* dissolution studies of cargo and PEGylated molecules. (A) *In vitro* dissolution profiles of PTX and VE-PTX (n = 3). PTX emulsions (PTX/VE/TPGS = 5/900/360, w/w); VE-PTX NEs (VE-PTX/VE/TPGS = 100/900/360, w/w); VE-PTX NEs using LA as the core (VE-PTX/LA/TPGS = 10/900/360, w/w). **(B)** *In vitro* DSPE-PEG2000-CF release from the NEs using the dialysis method (n = 3). The NEs of VE or oleic acid (VE or oleic acid/DSPE/DSPE-PEG/DSPE-PEG-CF=200/80/20/1, w/w) were prepared using the same method.
DSPE-PEG2000-CF: 1,2-distearoyl-sn-glycero-3-phosphoethanolamine-N-[poly(ethylene glycol)2000-N'-carboxyfluorescein]; LA: Linoleic acid; NE: Nanoemulsion; PTX: Paclitaxel; TPGS: D-α tocopheryl polyethylene glycol 1000 succinate; VE: Vitamin E; VE-PTX: Vitamin E-paclitaxel.

processing approaches. Preliminary treatment involved dissolving the individual components in chloroform that was then evaporated with a nitrogen gas flow. Trace amounts of chloroform were removed by keeping the mixtures under a vacuum in a desiccator for 1–2 h. For emulsions, some Zirconium Oxide beads (a third is 1.0 mm diameter and two-third is 0.5 mm diameter) and pH 7.4 phosphate buffer saline (PBS) were put into the Rino™ 1.5 ml screw-cap tube with the mixtures included. The mixtures were homogenized in the Bullet Blender (Next Advance, Inc.) set at the 8th speed for 8 min to form emulsions. To formulate the liposomes, the mixtures of lipids in the flask were dried as a thin layer and then hydrated in water while the temperature of the suspension was kept at approximately 80°C. The lipid dispersion was then sonicated for 2 min (probe sonicator, output power 10 W, Fisher Scientific). ^{3}H-labeled nanoformulations were prepared by mixing a trace amount of ^{3}H-PTX, ^{3}H-PTX-VE or ^{3}H-PTX-LA in the mixtures as preliminary treatment.

Transmission electron microscopy images

Transmission electron microscopy (TEM) images of all the NPs were acquired using a JEOL 100CX II TEM. Prepared samples (5 μl) were dropped onto a 200 mesh carbon-coated copper grid (Ted Pella, Inc., CA, USA) and allowed to stand for 5 min, and excess liquid was wicked off. Grids were then stained with 1% uranyl acetate (5 μl) for 10–15 sec and wicked dry. All images were acquired at an accelerating voltage of 100 kV.

In vitro release experiments

Dissolution profiles of PTX or VE-PTX from NEs were determined using dialysis technique. Two milliliters of NEs (5 mg/ml, calculated as PTX) were added in a dialysis membrane with a molecular weight cutoff of 12,000–14,000 Da, sealed from both ends and suspended in 200 ml of PBS solution or FBS (fetal bovine serum) solution under the agitation of 100 rpm using a paddle at 25°C. At predetermined time intervals (0, 0.5, 1, 2, 3, 4, 6, 8, 12, 24 and 32 h), 100 μl of medium was withdrawn and fresh medium was complemented. ^{3}H-labeled PTX and VE-PTX were quantified on a liquid scintillation analyzer (TRI-CARB, Packard Bioscience Company, MA, USA). *In vitro* DSPE-PEG2000-CF release from the NEs was determined using a similar method. The difference between the two methods was that the beaker was put in a shaker at 25°C. The samples were kept in the dark and analyzed using a fluorescence spectrophotometer (λ_{ex} = 450 nm, λ_{em} = 528 nm).

Pharmacokinetic experiments

Female CD-1 mice (18–22 g) received injections of 16 mg/kg of VE-PTX (or 10 mg/kg of PTX) into

the tail vein. Each mouse received 2 μCi of radiolabeled drugs. The volume injected into each mouse was approximately 0.2 ml. After injection, samples of 10–20 μg of blood was collected at each time point. Blood samples were digested in 0.2 ml of tissue solubilizer (Amersham Biosciences). Two-hundred microliters of 30% hydrogen peroxide was added to the samples for decolorization. A scintillation cocktail (Ultima Gold™ XR, PerkinElmer, MA, USA) was added to the decolorized samples and stored in the dark to allow any chemiluminescence to subside. The radioactivity was then quantified on a liquid scintillation analyzer (TRI-CARB, Packard Bioscience Company, MA, USA). The concentration of drugs in the samples was determined from the net intensity of radioactivity obtained by subtracting the intensity of radioactivity of the blank based on the standard calibration curve. Pharmacokinetic parameters were according to a noncompartmental PK model calculated by DAS 2.1.1 software.

Antitumor efficacy

To create the MDR tumor model, 5×10^6 KB-8–5 cells were injected subcutaneously into the right flanks of nude mice. Once the tumor mass in the xenograft was established, mice were randomly divided into different treatment groups and intravenously injected with different formulations of VE-PTX at a dose of 16 mg/kg (10 mg/kg PTX). The weight of the mice was monitored after they had received treatment. Tumor volume was calculated by the formula: (length × [width]^2)/2. Animals were treated in accordance with National Institute of Health Guide for the Care and Use of Laboratory Animals as approved by the University of North Carolina at Chapel Hill Institutional Animal Care and Use Committee.

In vivo distribution test

KB-8–5 tumor-bearing mice were intravenously injected with Taxol or molecular-matched VE-PTX NE at doses of 10 mg/kg. At 240 min after injection, animals were sacrificed and a kidney, lung, spleen, heart and 50–100 mg of liver and tumor were collected. The organs were washed twice with PBS and wiped. The samples were digested using tissue solubilizer, and quantified on liquid scintillation analyzer.

In vivo imaging

Free SRB and molecular-matched LA-SRB-loaded liposomes were intravenously injected through the tail vein of SKOV3 (human ovarian carcinoma cell) tumor-bearing mice (5 mg SRB/kg of or the same molar LA-SRB). The mice were imaged under anesthesia for several times after injection using a Kodak In-Vivo FXPro imaging system. The organs, including the heart, liver, spleen, lungs, kidneys, intestines, colon
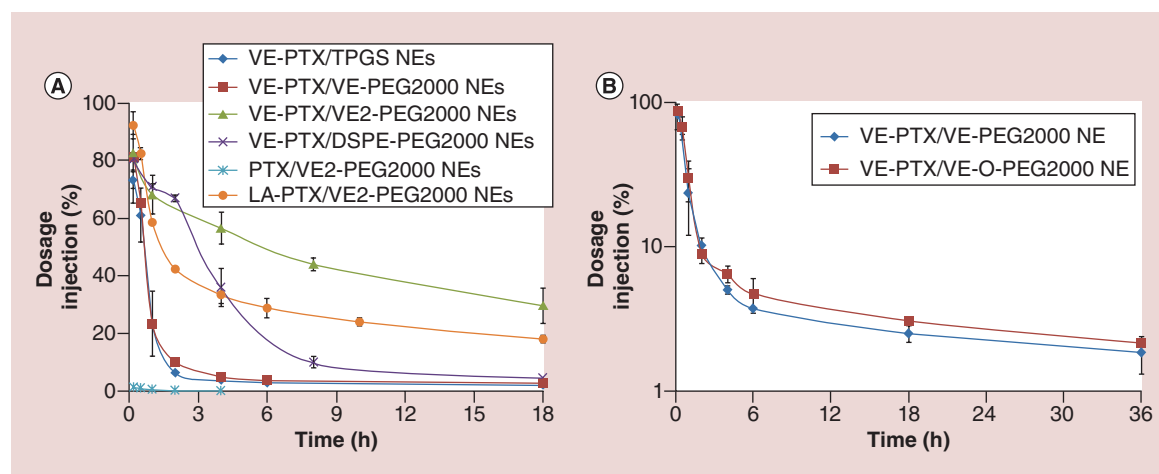

Figure 4. Pharmacokinetic studies of molecular-matched and molecular-mismatched emulsions. (A) The PK profiles of PTX emulsion and VE-PTX PEGylated NEs (n = 3). The mice were injected intravenously with different formulations (equal dose of 10 mg PTX/kg) containing 2 μCi ^{3}H labeled PTX (or ^{3}H labeled PTX-VE). PTX emulsions (PTX/VE/TPGS/VE$_2$-PEG2000 = 5/900/288/110, w/w); VE-PTX/TPGS NEs (VE-PTX/VE/TPGS = 100/900/340, w/w). All other VE-PTX PEGylated NEs contained the same molar ratio with VE-PTX/TPGS NEs, except that 20% mol TPGS was replaced with VE-PEG2000, DSPE-PEG2000 and VE$_2$-PEG2000. **(B)** PK comparison between VE-PTX NEs PEGylated with VE-O-PEG2000 and VE-PEG2000 (n = 3). The mice were injected intravenously with the dose of 16 mg VE-PTX/kg containing 2 μCi ^{3}H labeled PTX-VE. VE-PTX NEs (VE-PTX/VE/TPGS/VE2-(O)-PEG2000 = 100/900/288/90, w/w).
DSPE-PEG2000: 1,2-distearoyl-sn-glycero-3-phosphoethanolamine-N-[amino(polyethylene glycol)-2000];
NE: Nanoemulsion; PK: Pharmacokinetic; PTX: Paclitaxel; TPGS: D-α tocopheryl polyethylene glycol 1000 succinate;
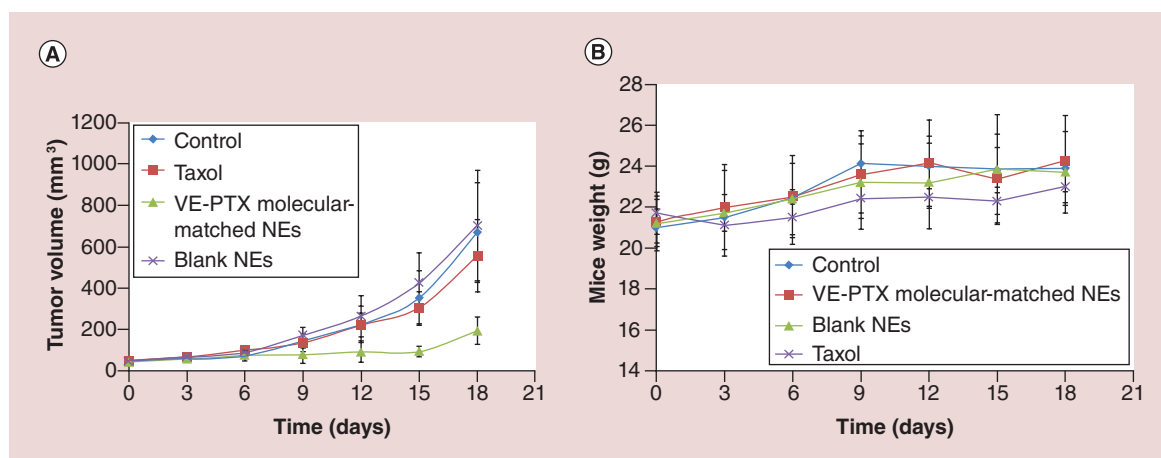VE: Vitamin E; VE-PTX: Vitamin E-paclitaxel.

Figure 5. Antitumor effects in KB-8–5 multiple drug resistance tumor-bearing mice. The mice were intravenously injected with the VE-PTX NEs or Taxol or blank NEs every 3 days for five consective injections. The tumor volume **(A)** and the mice weight **(B)** were determined (the mice were sacrificed 18 days after the first injection). The VE-PTX NEs were formulated with VE-PTX/VE/TPGS/VE_2-PEG2000=100/900/288/110 (w/w).
#No significant difference; *p < 0.05; **p < 0.01 (n = 5).
NE: Nanoemulsion; TPGS: D-α tocopheryl polyethylene glycol 1000 succinate; VE: Vitamin E; VE-PTX: Vitamin E-paclitaxel.

and tumor were collected 8 h after injection and also imaged.

Results & discussion
Increased compatibility between PTX & VE by the MMMs

Among the biocompatible oils, tocopherol (VE) has a relatively high capacity to dissolve PTX. This discovery led to the development of the injectable PTX NEs from Sonus Pharmaceuticals. However, despite an ability to dissolve PTX, the PK from these NEs demonstrated that VE was not able to retain PTX within the core. This led to a rapid loss of PTX from the system and consequently poor efficacy. Consequently, solubility alone is not highly predictive of PK outcomes. Drug partitioning is a ratio of favorability between the two phases comprising an interface. Thus drug retention will depend on maximizing the favorability for the emulsion core compared with water, protein surfaces and cell membranes from endothelial cells or erythrocytes. To prove the concept that the compatibility between PTX and VE can be enhanced through the MMMs, we conjugated PTX to VE or LA (Figure 2A). The solubility of PTX as well as the VE–PTX and LA–PTX conjugates in either VE or LA was examined. The solubility of PTX in VE and LA was 46.6 and 2.8 μmol/ml, respectively. As PTX was conjugated with VE or LA, the solubility increased to 298.7 μmol/ml (VE-PTX in VE) and 21.0 μmol/ml (LA-PTX in LA). The enhanced solubility demonstrates the molecular-matched pattern: the increased solubility of VE-PTX in VE greater than VE-PTX in LA and the solubility of LA-PTX in LA greater than LA-PTX

in VE (Figure 2B). The molecular-matched NEs were formulated to deliver the molecular-matched prodrug (VE-PTX), with an encapsulation efficiency of >98% and a particle size of 70.5 ± 4.8 nm (Figure 2C & D). In contrast, the VE emulsion carrying free PTX showed both large-size particles and crystal precipitation (Figure 2E). The molecular-matched NEs were stable in a week at an ambient temperature (no precipitation and no change in particle size), and even remained a transparent solution after 3 months of storage at 4°C. The VE emulsion on the other hand becomes turbid.

Controlled release & minimized PEG-shedding by the MMMs

To efficiently deliver a drug to the tumor tissues, NPs must compactly house the loaded drugs during circulation with minimal or no drug release. We hypothesized that the stability of PTX in the VE cores could be greatly improved through the use of the MMMs technique because of a decreased crystallinity of the PTX-VE prodrug and improved interactions between the core and the molecular-matched conjugates. As shown in Figure 3A, a quick release of PTX from the VE NEs was observed; the accumulated PTX that was released in PBS reached 50% in 8 h. However, <2% of the molecular-matched VE-PTX NEs in PBS and <3% of the molecular-matched VE-PTX NEs in 5% FBS were released in 32 h. As expected, mismatched VE-PTX in LA NEs was released more quickly than the correctly matched VE-PTX in VE NEs. These data indicate that stable drug-residence and adjustable drug release can be achieved using the MMMs.

In addition to obtaining stable drug residence in the NPs, the retention of the PEG coating on the surface of NPs is also important. The dissociation of PEG derivatives (shedding) from the liposomal membrane was first reported by Cullis [18]. To assess if using MMMs could minimize PEG shedding *in vitro*, the core of the NEs was adjusted to match (or mismatch) the two 18-carbon tails of DSPE-PEG2000-CF (carboxyfluorescein) (Avanti Polar Lipid) and the amount of dissociation of the DSPE-PEG2000-CF was determined. As shown in Figure 3B, less than 2% of PEG shedding in PBS was detected for both the molecular-matched (oleic acid as the core) and mismatched (VE as the core) PEGylated NEs. In 5% FBS, increased shedding of PEG was observed, but the molecular-matched PEGylated NEs exhibited a shedding of PEG that was much slower than that of the mismatched PEGylated NEs (17 vs 57% release in 32 h).

Manipulate the PK of NEs with molecular-matched & molecular-mismatched agents

To assess if the PK of loaded PTX or VE-PTX in PEGylated NEs could be improved using the MMMs, we conjugated VE to PEG, creating VE-PEG2000 and VE$_2$-PEG2000, which contained two VE tails. When free PTX was carried by the emulsion PEGylated with the VE$_2$-PEG2000, the PK was much shorter than that of any VE-PTX PEGylated NEs (Figure 4A). This was attributed to poor compatibility between PTX and VE. The PK of the VE-PTX NEs PEGylated with VE$_2$-PEG (molecular-matched, two VE tails) was much longer than those of the VE-PTX NEs PEGylated with DSPE-PEG2000 (mismatched, two lipid tails) and VE-PEG2000 (molecular-matched, a VE tail). These data indicate, in addition to the molecular-matched, the two lipid-tails of the PEG
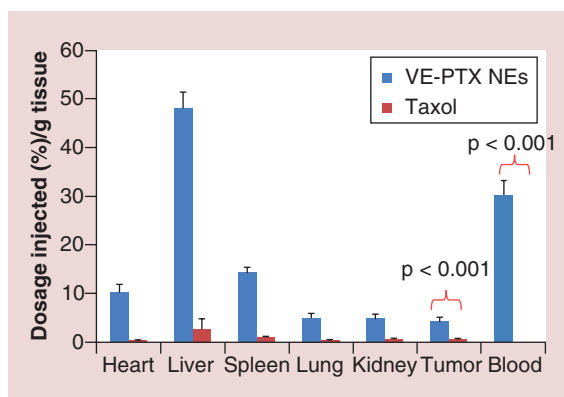

Figure 6. *In vivo* biodistribution of Taxol and VE-PTX molecular-matched NEs (VE-PTX/VE/TPGS/VE$_2$-PEG2000=100/900/288/110, w/w) at 6 h postinjection in KB-8–5 tumor-bearing mice (n = 5).
NE: Nanoemulsion; TPGS:D-α tocopheryl polyethylene glycol 1000 succinate; VE: Vitamin E; VE-PTX: Vitamin E-paclitaxel.

derivatives may prolong the PK more efficiently than a single lipid-tail, putatively because of increased interactions with the particle core. We also loaded LA-PTX as a molecular-mismatched cargo in the VE core of the NEs PEGylated with the VE$_2$-PEG2000 and examined its PK. As the molecular-matched VE-PTX was replaced by molecular-mismatched LA-PTX, the PK of the LA-PTX NE became shorter than that of VE-PTX NEs. This further confirms the molecular-matched cargo plays an important role in cargo retention. All the data above demonstrate that the desired PK can be achieved by modifying both the lipid anchor of the PEG derivatives and the therapeutic (or imaging) agents to be molecular-matched to the carrier. It also suggests the possibility of designing the NEs with a tunable PK using the MMMs (Table 1). Additionally, we synthesized VE-O-PEG2000, in which VE was

Table 1. Pharmacokinetic parameters of paclitaxel and vitamin E-paclitaxel and linoleic acid-paclitaxel after intravenous injection (n = 3).						
Parameters	VE$_2$-PEG2000 NEs	DSPE-PEG2000 NEs	VE$_2$-PEG2000 NEs	VE-PEG2000 NEs	TPGS NEs	VE$_2$-PEG2000 NEs
	VE-PTX	VE-PTX	LA-PTX	VE-PTX	VE-PTX	PTX
AUC$_{(0-t)}$ (mg/l h)	2220.94 ± 199.37	1414.86 ± 104.39	2596.68 ± 295.4	379.67 ± 60.38	313.20 ± 25.39	6.17 ± 2.35
AUC$_{(0-\infty)}$ (mg/l h)	3208.76 ± 117.10	1415.41 ± 104.3	3397.68 ± 1036.62	381.64 ± 60.52	315.7 ± 25.84	6.38 ± 2.44
MRT$_{(0-t)}$ (h)	7.2536 ± 0.24	9.71 ± 0.32	16.62 ± 0.55	3.69 ± 0.11	3.31 ± 0.09	1.24 ± 0.04
MRT$_{(0-\infty)}$ (h)	15.51 ± 1.29	9.72 ± 0.33	31.70 ± 14.04	3.79 ± 0.11	3.45 ± 0.11	1.45 ± 0.08
t$_{1/2}$ (h)	10.99 ± 0.94	4.26 ± 0.13	23.97 ± 10.60	2.81 ± 0.09	3.23 ± 0.11	1.30 ± 0.11
CL (l/h/kg)	0.004 ± 0.000	0.010 ± 0.001	0.004 ± 0.001	0.036 ± 0.006	0.043 ± 0.004	2.351 ± 0.972
V$_D$ (l/kg)	0.07 ± 0.01	0.06 ± 0.01	0.13 ± 0.02	0.15 ± 0.03	0.20 ± 0.01	4.49 ± 1.95
C$_{max}$ (mg/l)	220.52 ± 13.79	217.27 ± 20.27	248.76 ± 8.11	216.07 ± 39.24	199.11 ± 8.25	4.51 ± 1.35
CL: Total body clearance; DSPE-PEG2000: 1,2-distearoyl-sn-glycero-3-phosphoethanolamine-N-[amino(polyethylene glycol)-2000]; MRT: Mean retention time; NE: Nanoemulsion; t$_{1/2}$: Half-life; TPGS: D-α tocopheryl polyethylene glycol 1000 succinate; VD: Volume of distribution; VE: Vitamin E.						

Table 2. Kidney and liver function parameters in the different experimental group (n = 5).			
Formulation	AST(U/l)	ALT(U/l)	BUN/(mg/dl)
Control	133.8 ± 9.7	65.8 ± 17.3	22.4 ± 1.5
Taxol	217.2 ± 54.4	99.2 ± 19.4	24.6 ± 1.5
PTX-VE NEs	125.9 ± 23.2*	57.6 ± 3.5*	23.6 ± 2.5
Normal range	54–298	17–77	8–33
*p < 0.01 Values are given as mean ± standard deviation. Serum samples were collected after mice received four-times 10 mg/kg Taxol or 16 mg/kg VE-PTX NEs every other day. ALT: Alanine aminotransferase; AST: Aspartate aminotransferase, BUN: Blood urea nitrogen; VE-PTX: Vitamin E-paclitaxel.			

linked to PEG2000 through an ether bond. An ether bond is more biologically stable than an ester bond. The NEs PEGylated with VE-O-PEG2000 showed a similar PK to that of the ester bond linked VE-PEG2000 (Figure 4B), indicating that de-PEGylation of the NEs is due to the PEG derivatives shedding, not the ester bond hydrolysis.

Deliver the molecular-matched NEs to treat multidrug resistance in cancer

The molecular-matched NEs have an ability to circulate for a long time leading to preferential accumulation of the NE within the tumor tissues via the enhanced permeability and retention (EPR) effect. To evaluate the *in vivo* antitumor efficacy, KB-8–5 MDR tumor-bearing mice were intravenously injected with the VE-PTX NEs or Taxol every 3 days. The administration of Taxol did not induce any noticeable inhibition of MDR tumor growth (Figure 5A). A significant regression of MDR tumors was observed in mice treated with the VE-PTX

NEs, indicating that the VE-PTX NEs using VE as the core can efficiently sensitize MDR tumors. The significant *in vivo* efficacy might be explained by two occurrences: one is the enhanced accumulation of molecular-matched NEs at the tumor site due to long circulation (Figure 6), and second that VE and TPGS could induce a significant reversal of MDR. In fact, we found that VE is the key structure of TPGS, responsible for inhibiting P-gp [19]. As for tolerability, no weight loss occurred in the mice treated with the VE-PTX NEs (Figure 5B). Changes in the serum aspartate aminotransferase, alanine aminotransferase and blood urea nitrogen levels, which are commonly used as biochemical markers for liver and kidney function, were also examined. The alanine aminotransferase and aspartate aminotransferase were significantly elevated in the group treated with Taxol but not with the VE-PTX NEs (Table 2). Taken together, the results indicated that in addition to increased efficacy and MDR sensitization, the VE-PTX NEs are much better tolerated than Taxol.
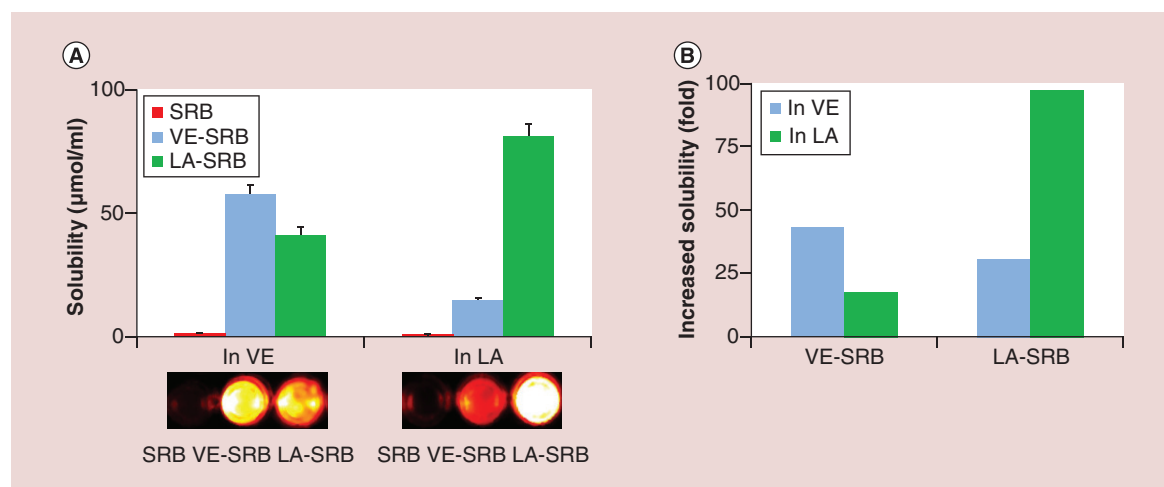

Figure 7. The solubilities of hydrophilic fluorescent imaging molecule, sulforhodamine acid chloride and its conjugates. (A) Solubility of SRB and SRB conjugates in VE or LA (top) and imaging of the saturated solution (bottom). The solubility of free SRB, the conjugates of VE-SRB and LA-SRB were quantified using a fluorescence spectrophotometer (λ_{ex} = 560 nm, λ_{em} = 584 nm). Photos were taken of the saturated solutions of VE and LA containing free SRB or the conjugates. **(B)** Increase in solubility of SRB conjugates compared with free SRB. LA: Linoleic acid; SRB: Sulforhodamine acid chloride; VE: Vitamin E.
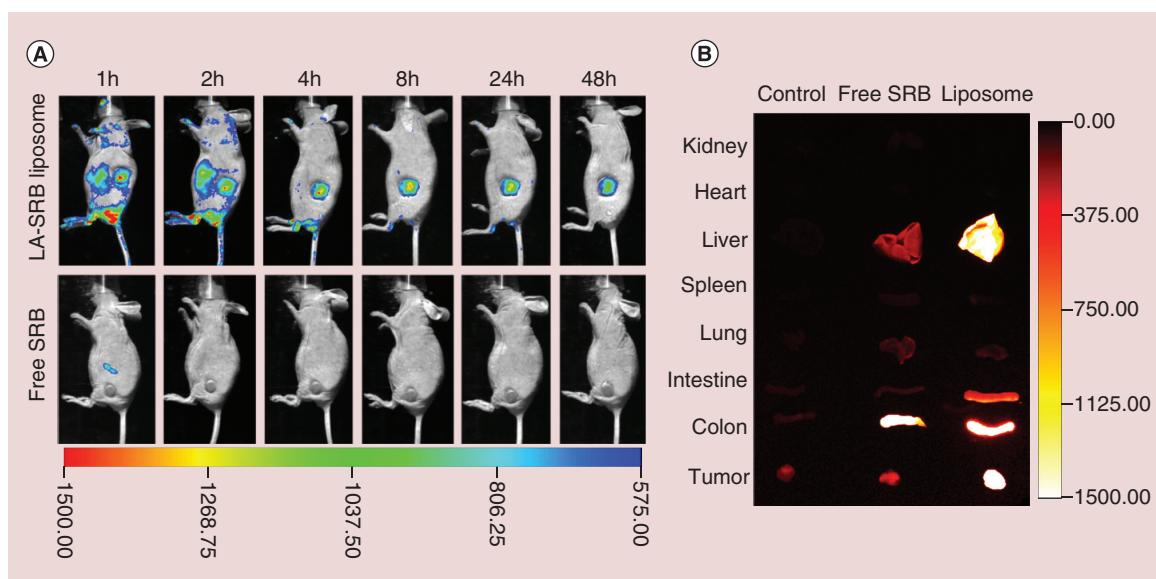
Figure 8. *In vivo* images of free SRB and LA-SRB molecular-matched liposomes (DOPC/LA/DSPE-PEG2000/LA-SRB =1000/500/280/80, w/w). The mice were injected intravenously with either free SRB or LA-SRB molecular-matched liposomes (5 mg SRB/kg). Photos were taken at the indicated time-points using the Kodak *In-Vivo* FXPro imaging system (λ_{ex} = 500nm, λ_{em} = 600nm) **(A)**. *Ex vivo* biodistribution of free SRB and LA-SRB molecular-matched liposomes in mice. The mice were sacrificed 8 h after injection and the organs were collected and imaged **(B)**. DOPC: 1,2-dioleoyl-sn-glycero-3-phosphocholine; DSPE-PEG2000: 1,2-distearoyl-sn-glycero-3-phosphoethanolamine-N-[amino(polyethylene glycol)-2000]; LA: Linoleic acid; SRB: Sulforhodamine acid chloride.

Establish molecular-matched liposome to deliver water soluble fluorophore for tumor-imaging

To assess if the compatibility between hydrophilic molecules and oil can be also enhanced using the MMMs, a water-soluble SRB was conjugated to VE or LA. As shown in Figure 7A, the solubility of SRB in oil was improved by the conjugation, which increased from 0.77 µmol/ml (SRB) to 33.2 µmol/ml (VE-SRB) in VE and increased from 0.48 µmol/ml (SRB) to 46.7 µmol/ml (LA-SRB) in LA. The enhanced solubility also showed the core-dependence (Figure 7B), i.e., the solubility of VE-SRB in VE > in LA (33.2 vs 8.4 µmol/ml) and LA-SRB in LA > in VE (46.7 vs 23.6 µmol/ml).

We also developed molecular-matched liposomes using the MMMs for tumor imaging. Very few studies have reported the successful encapsulation of water-soluble fluorophores in liposomes for the purpose of *in vivo* imaging of tumors. The low-loading efficiency is most likely the cause of this setback. Improving the affinity and compatibility of SRB to the LA lipid using the MMMs allows us to encapsulate LA-SRB in liposomes for imaging of tumors. The molecular-matched liposomes were prepared through the inclusion of LA in the liposomes to provide the molecular-matched environment for LA-SRB. The particle size of LA-SRB liposomes remained unchanged (110.5 ± 7.7 nm) at 4°C after 1 month of storage. Whole-body imaging in tumor-bearing mice (Figure 8A) showed that no fluorescence was detectable in the tumors after injection with free SRB. However, the SRB signal was detected in the tumors 1 h after the injection of the molecular-matched liposomes. The detectable florescent-signal in the tumors lasted for as long as 2 days postinjection (no signal was detected on day 3). While the colon and liver were the major organs taking up the liposomes (Figure 8B), the whole-body imaging failed to detect this pattern because of the shallow tissue penetration of fluorescence imaging. The light tissue penetration can be improved using a near-infrared fluorescent dye, such as indocyanine green.

Conclusion

Rationally designed nanocarriers would benefit from an ability to carry both hydrophobic and hydrophilic bioactive materials, prevent drugs from interacting with the biological environment during circulation and control the PK and drug release profiles. The presented molecular-matched NPs have demonstrated high-drug loading capacity for hydrophobic drugs as well as a hydrophilic imaging probe. The MMMs also could be applied to maintain stable residence of both the drugs and probes within the core during circulation. Furthermore, the development of molecular-matched NPs based on MMMs emphasizes the importance of 'matching' to the stability of the NPs.

Future perspective

The developed NEs are composed of entirely generally recognized as safe materials to facilitate the clinical translation of the delivery systems. While the molecular-matched conjugates of the VE-PTX (prodrug) and VE-PEG reported here are new derivatives, they are not new chemical entities. The VE, PTX and PEG derivatives are currently being used clinically. The reformulation of these MMMs may provide a powerful tool to improve the disposition of drugs without affecting clinical translation. More importantly, the MMMs show the versatility to be utilized in the design of tailored, multifunctional theranostic NPs, which could be even more valuable as this nascent field begins to grow in importance.

Dedication

This paper is dedicated to the memory of Professor Feng Liu, PhD, 1955–2014 University of North Carolina at Chapel Hill, NC, USA.

Ethical conduct of research

The authors state that they have obtained appropriate institutional review board approval or have followed the principles outlined in the Declaration of Helsinki for all human or animal experimental investigations. In addition, for investigations involving human subjects, informed consent has been obtained from the participants involved.

Executive summary

Background
- The compatibility between the cargo and the core of the nanoparticles should be emphasized to investigate as designing nanomedicine.

Materials & methods
- Molecular-matched materials are established through the conjugation of the functional moiety to a molecule representative of the nanoparticle's core.

Results & discussion
- The developed nanoemulsion using molecular-matched materials showed good *in vitro* stability.
- The molecular-matched PEGylated nanoemulsions (NEs) exhibited a shedding of PEG that was much slower than that of the mismatched PEGylated NEs.
- The pharmacokinetics of the cargo encapsulated in the nanoparticles could be manipulated through adjusting the compatibility between the core of the nanoparticles and the drug or PEGylated molecule.
- Enhanced accumulation of molecular-matched nanoemulsions at the tumor site was achieved due to the long circulation characteristics of the NEs.
- Vitamin E-paclitaxel NEs using vitamin E as the core can efficiently sensitize multiple drug resistance tumors when compared with Taxol.
- The established molecular-matched liposome also showed good *in vivo* imaging ability.

References

Paper of special note have been highlighted as: • of interest

1   Ashley CE, Carnes EC, Phillips GK *et al.* The targeted delivery of multicomponent cargos to cancer cells by nanoporous particle-supported lipid bilayers. *Nat. Mater.* 10(5), 389–397 (2011).

2   Liu Y, Fang J, Kim YJ, Wong MK, Wang P. Codelivery of doxorubicin and paclitaxel by cross-linked multilamellar liposome enables synergistic antitumor activity. *Mol. Pharm.* 11(5), 1651–1661 (2014).

3   Yu Z, Schmaltz RM, Bozeman TC *et al.* Selective tumor cell targeting by the disaccharide moiety of bleomycin. *J. Am. Chem. Soc.* 135(8), 2883–2886 (2013).

4   Yang C, He X, Song L *et al.* Gamma-Fe$_2$O$_3$ nanoparticles increase therapeutic efficacy of combination with paclitaxel and anti-ABCG2 monoclonal antibody on multiple myeloma cancer stem cells in mouse model. *J. Biomed. Nanotech.* 10(2), 336–344 (2014).

5   Singodia D, Talegaonkar S, Khar RK, Mishra PR. Novel polymer coupled lipid nanoparticle of paclitaxel with synergistic enhanced efficacy against cancer. *J. Biomed. Nanotech.* 7(1), 125–126 (2011).

6   Rabinow BE. Nanosuspensions in drug delivery. *Nat. Rev. Drug Discov.* 3(9), 785–796 (2004).

7   Singla AK, Garg A, Aggarwal D. Paclitaxel and its formulations. *Int. J. Pharm.* 235, 179–192 (2002).

8   Tije AJ, Verweij J, Loos WJ, Sparreboom A. Pharmacological effects of formulation vehicles: implications for cancer chemotherapy. *Clin. Pharmacokinet.* 42, 665–685 (2003).

9   Fu S, Naing A, Moulder SL *et al.* Phase I trial of hepatic arterial infusion of nanoparticle albumin-bound paclitaxel: toxicity, pharmacokinetics, and activity. *Mol. Cancer Therapeut.* 10(7), 1300–1307 (2011).

10 Okamoto I, Yamamoto N, Kubota K *et al.* Safety and pharmacokinetic study of nab-paclitaxel plus carboplatin in chemotherapy-naive patients with advanced non-small cell lung cancer. *Invest. New Drugs* 30(3), 1132–1137 (2012).

11 Perez EA. Novel enhanced delivery taxanes: an update. *Semin. Oncol.* 34(3), suppl 1–5 (2007).

12 Letchford K, Burt HM. Copolymer micelles and nanospheres with different *in vitro* stability demonstrate similar paclitaxel pharmacokinetics. *Mol. Pharm.* 9(2), 248–260 (2011).

•   **Highlights the importance of the compatibility between drug and its carriers.**

13 Ke XY, Zhao BJ, Zhao X *et al.* The therapeutic efficacy of conjugated linoleic acid – paclitaxel on glioma in the rat. *Biomaterials* 31(22), 5855–5864 (2010).

14 Ma Y, Liu D, Wang D *et al.* Combinational delivery of hydrophobic and hydrophilic anticancer drugs in single nanoemulsions to treat MDR in cancer. *Mol. Pharm.* 11(8), 2623–2630 (2014).

15 Yang X, Wang D, Ma Y *et al.* Theranostic nanoemulsions: codelivery of hydrophobic drug and hydrophilic imaging probe for cancer therapy and imaging. *Nanomedicine (Lond.)* 1–13 (2014).

16 Danhier F, Kouhe TT, Duhem N *et al.* Vitamin E-based micelles enhance the anticancer activity of doxorubicin. *Int. J. Pharm.* 476(1–2), 9–15 (2014).

17 Wang J, Sun J, Chen Q *et al.* Star-shape copolymer of lysine-linked di-tocopherol polyethylene glycol 2000 succinate for doxorubicin delivery with reversal of multidrug resistance. *Biomaterials* 33(28), 6877–6888 (2012).

18 Parr MJ, Ansell SM, Choi LS, Cullis PR. Factors influencing the retention and chemical stability of poly(ethylene glycol)-lipid conjugates incorporated into large unilamellar vesicles. *Biochim. Biophys. Acta* 1195(1), 21–30 (1994).

19 Tang J, Fu Q, Wang Y, Racette K, Wang D, Liu F. Vitamin E reverses multidrug resistance *in vitro* and *in vivo*. *Cancer Lett.* 336(1), 149–157 (2013).

•   **Points out that the vitamin E is the key structure of tocopheryl polyethylene glycol 1000 succinate in reversing multiple drug resistance.**